

Moment-Fourier approach to ion parallel fluid closures and transport for a toroidally confined plasma

Jeong-Young Ji,^{*} Eric D. Held, and J. Andrew Spencer

Department of Physics, Utah State University, Logan, Utah 84322, USA

Yong-Su Na

Department of Nuclear Engineering,

Seoul National University, Seoul 08826, South Korea

Abstract

A general method of solving the drift kinetic equation is developed for an axisymmetric magnetic field. Expanding a distribution function in general moments a set of ordinary differential equations are obtained. Successively expanding the moments and magnetic-field involved quantities in Fourier series, a set of linear algebraic equations is obtained. The set of full (Maxwellian and non-Maxwellian) moment equations is solved to express the density, temperature, and flow velocity perturbations in terms of radial gradients of equilibrium pressure and temperature. Closure relations that connect parallel heat flux density and viscosity to the radial gradients and parallel gradients of temperature and flow velocity, are also obtained by solving the non-Maxwellian moment equations. The closure relations combined with the linearized fluid equations reproduce the same solution obtained directly from the full moment equations. The method can be generalized to derive closures and transport for an electron-ion plasma and a multi-ion plasma in a general magnetic field.

^{*} j.ji@usu.edu

I. INTRODUCTION

For magnetically confined plasmas, neoclassical transport theory describes particle, heat, and momentum transport of a steady-state plasma due to Coulomb collisions in an inhomogeneous magnetic field [1–7]. The neoclassical transport is obtained by solving the first order drift kinetic equation [8, 9] assuming a zeroth order background distribution (see Ref. [10, 11] for reviews). Due to difficulty in treating the integro-differential collision operator in velocity space, modified collision operators have been adopted for analytical work. Numerical work may adopt the Landau (Fokker-Planck) collision operator with desired accuracy by increasing velocity space resolution. Numerous transport codes have been developed to solve the continuum drift kinetic equation with a modified [12, 13] or an exact Landau collision operator [14–19].

For describing a macroscopic state of a tokamak plasma, the fluid variables are of primary importance and solving fluid equations instead of the kinetic equation may be sufficient. Due to significantly lower dimensionality of position space compared to phase space, numerically solving fluid equations has a great advantage over solving the kinetic equation [20–24]. The key issue is to obtain proper closures to capture desired physics effects. Even though the heat flux density is derived in neoclassical transport theory, it cannot serve as one of closures for the temperature equation because it is derived from the fluid equations, and hence, expressed in terms of the zeroth-order density and temperature instead of the (first-order) fluid variables whose evolution equations are to be closed. That is, the heat flux derived from the divergence free condition plays no role for the divergence term in the temperature equation.

In this work, we introduce an analytic method to solve the drift kinetic equation to obtain closures and transport. For a magnetized plasma, the parallel moment equations are derived in Ref. [25]. One advantage of the moment approach is the availability of the exact collisional moments of the linearized Landau operator [26]. The moment-based collision operator can be utilized for the linear and nonlinear gyrokinetic Coulomb collision operator [27–29]. For slab geometry where the magnetic field strength does not change along a magnetic field line, the drift-kinetic equation can be converted to a linear system of ordinary differential equations with constant coefficients. This linear system can be analytically solved for the

parallel moments using the eigenvector method [30].

On the other hand, for an inhomogeneous magnetic field of a tokamak, the drift kinetic equations becomes a linear system of ordinary differential equations with varying coefficients. This means that the eigenvector method used in the integral closure [30] does not work. For a system of linear differential equations with varying coefficients, we can Fourier-expand the varying coefficients and moments to build a system of linear algebraic equations. While truncation both in the moments and Fourier modes is inevitable, the solution of the truncated system is equivalent to that of the drift kinetic equation when convergence is achieved by increasing the number of moments and Fourier modes. The solution moments can then be used to construct the distribution function that is the solution of the drift kinetic equation. Therefore the moment solution can be used for benchmarking numerous fluid and kinetic codes.

In Sec. II, we present the parallel moment equations which are equivalent to the first order drift kinetic equation. In Sec. III, we use the Fourier expansion to solve the general moment equations for fluid quantities in Fourier series. The convergent solution is presented as the numbers of moments and Fourier modes increase. In Sec. IV, we derive closures and incorporate them into fluid equations to reproduce the fluid quantities. In Sec.V, we conclude and discuss possible extensions of the work to more general plasmas.

II. DRIFT KINETIC EQUATION AND MOMENT EQUATIONS

In standard neoclassical transport theory (see Ref. [11] for a general review), drift kinetic equations are solved for ion and electron transport. An analytic solution can be obtained for an axisymmetric magnetic field

$$\mathbf{B} = I\nabla\zeta + \nabla\zeta \times \nabla\psi \quad (1)$$

where $2\pi\psi$ is the poloidal flux, $2\pi I/\mu_0$ is the poloidal current, μ_0 is the magnetic permeability, and ζ is the toroidal angle. For simplicity, we assume a circular magnetic field

$$B = \frac{B_0}{1 + \epsilon \cos \theta} \quad (2)$$

where θ is the poloidal angle, B_0 is a constant reference field, $\epsilon = r/R_0$ is the inverse aspect ratio, and R_0 and r respectively are the major and minor radii of a circular-shape flux surface.

For ion transport, the ion-electron collisions are often ignored and the reduced ion drift kinetic equation for the first-order distribution function f_1 becomes

$$v_{\parallel} \partial_{\parallel} (f_1 - F) = C(f_1) \quad (3)$$

with

$$F = -\frac{Iv_{\parallel}}{\Omega} \frac{df_0}{d\psi} = -\frac{Iv_{\parallel}}{\Omega} \left[\frac{d \ln p_0}{d\psi} + \left(s^2 - \frac{5}{2} \right) \frac{d \ln T_0}{d\psi} \right] f_0 \quad (4)$$

and

$$f_0(\psi, w) = \frac{n_0(\psi)}{[2\pi m T_0(\psi)]^{3/2}} e^{-w/T_0(\psi)} = \frac{n_0}{\pi^{3/2} v_0^3} e^{-s^2} \quad (5)$$

in the $(\psi, \theta, w = mv^2/2, \mu = mv_{\perp}^2/2B)$ coordinates, where $\partial_{\parallel} = \mathbf{b} \cdot \nabla = (\mathbf{B}/B) \cdot \nabla$, $v_{\parallel} = \mathbf{b} \cdot \mathbf{v}$, $\Omega = qB/m$, $v_0 = \sqrt{2T_0/m}$, and $s = v/v_0$. Note that flux surfaces can be labeled by the lowest-order density n_0 , temperature T_0 , or pressure $p_0 = n_0 T_0$. The collision operator is a Landau operator linearized with respect to a static Maxwellian distribution function f_0 ,

$$C(f_1) = C(f_1, f_0) + C(f_0, f_1). \quad (6)$$

One difficulty of solving the kinetic equation (3) is in treating the collision operator, an integro-differential operator in velocity space. In standard analytical neoclassical theory, the Landau operator is often approximated as the Lorentz pitch-angle scattering operator with an additional momentum restoring term for an analytical treatment. In the moment approach, the linearized collision operator can be analytically calculated and explicitly represented by a matrix of collision coefficients. In this work, we solve a system of parallel moment equations introduced in Ref. [25, 26]. The moment equations can also be derived from the drift kinetic equation as shown below.

In the moment method of this work, a gyro-averaged distribution function f_1 is expanded as

$$f_1 = f_0 \sum_{l,k} \hat{P}^{lk} \hat{M}^{lk} \quad (7)$$

with orthonormal polynomials

$$\hat{P}^{lk} = \frac{1}{\sqrt{\bar{\sigma}_{lk}}} P^{lk} = \frac{1}{\sqrt{\bar{\sigma}_{lk}}} s^l P_l(v_{\parallel}/v) L_k^{(l+1/2)}(s^2),$$

where P_l is a Legendre polynomial, $L_k^{(l+1/2)}$ is an associated Laguerre (Sonine) polynomial, and the normalization constants are

$$\bar{\sigma}_{lk} = \bar{\sigma}_l \lambda_{lk}, \quad \bar{\sigma}_l = \frac{1}{2l+1}, \quad \lambda_{lk} = \frac{(l+k+1/2)!}{k!(1/2)!}. \quad (8)$$

Several lowest order moments of f_1 are: $\hat{M}^{00} = n_1/n_0$ (density), $\hat{M}^{01} = -\sqrt{3/2}T_1/T_0$ (temperature), $\hat{M}^{10} = \sqrt{2}u/v_0$ (parallel flow velocity $u = V_{1\parallel}$), $\hat{M}^{11} = -\sqrt{4/5}h_{\parallel}/v_0p_0$ (parallel heat flux density), and $\hat{M}^{20} = \sqrt{3/4}\pi_{\parallel}/p_0$ (parallel viscosity), where $p_0 = n_0T_0$. The neoclassical thermodynamic drive term can also be expanded as

$$\begin{aligned} v_{\parallel} \partial_{\parallel} F = & \frac{v_0 \partial_{\parallel} \ln B}{B/B_0} f_0 \left[\left(2\hat{P}^{00} - 2\sqrt{\frac{2}{3}}\hat{P}^{01} + \frac{1}{\sqrt{3}}\hat{P}^{20} \right) \hat{p}_{0,\psi} \right. \\ & \left. + \left(-5\sqrt{\frac{2}{3}}\hat{P}^{01} + 2\sqrt{\frac{10}{3}}\hat{P}^{02} + \frac{1}{\sqrt{3}}\hat{P}^{20} - \sqrt{\frac{7}{6}}\hat{P}^{21} \right) \hat{T}_{0,\psi} \right], \end{aligned} \quad (9)$$

where

$$\hat{p}_{0,\psi} = \frac{I}{qv_0 B_0 n_0} \frac{dp_0}{d\psi}, \quad (10)$$

$$\hat{T}_{0,\psi} = \frac{I}{qv_0 B_0} \frac{dT_0}{d\psi}. \quad (11)$$

Taking the \hat{P}^{jp} moment of Eq. (3) yields

$$\sum_{lk} \psi^{jp,lk} \partial_{\parallel} \hat{M}^{lk} + \psi_B^{jp,lk} (\partial_{\parallel} \ln B) \hat{M}^{lk} = \frac{1}{\lambda_C} c^{jp,lk} \hat{M}^{lk} + \frac{\partial_{\parallel} \ln B}{B/B_0} \left(g_p^{jp} \hat{p}_{0,\psi} + g_T^{jp} \hat{T}_{0,\psi} \right), \quad (12)$$

where $\lambda_C = v_0 \tau_{ii}$ (the ion mean free path). Note that eliminating $(j, p) = (0, 0)$, $(0, 1)$, and $(1, 0)$ moment equations from Eq. (12) yields a set of closure moment equations, similar to the closure moment equations in slab geometry Ref. [31]. The constant coefficients $\psi^{jp,lk}$, $\psi_B^{jp,lk}$, and $c^{jp,lk}$ are defined by

$$\int d^3v v_{\parallel} \hat{P}^{jp} \hat{P}^{lk} f_0 = n_0 v_0 \psi^{jp,lk}, \quad (13)$$

$$\int d^3v v_{\parallel} \hat{P}^{jp} (\partial_{\parallel} \hat{P}^{lk}) f_0 = n_0 v_0 (\partial_{\parallel} \ln B) \psi_B^{jp,lk}, \quad (14)$$

$$\int d^3v \hat{P}^{jp} C(f_0 \hat{P}^{lk}) = \frac{n_0}{\tau_{ii}} c^{jp, lk} = \frac{n_0}{\tau_{ii}} \delta_{jl} c_{pk}^j. \quad (15)$$

The nonvanishing g^{jp} in Eq. (9) are

$$g_p^{0,0} = 2, \quad g_p^{0,1} = -2\sqrt{\frac{2}{3}}, \quad g_p^{2,0} = \frac{1}{\sqrt{3}} \quad (16)$$

and

$$g_T^{0,1} = -5\sqrt{\frac{2}{3}}, \quad g_T^{0,2} = 2\sqrt{\frac{10}{3}}, \quad g_T^{2,0} = \frac{1}{\sqrt{3}}, \quad g_T^{2,1} = -\sqrt{\frac{7}{6}}. \quad (17)$$

Noting that $\psi^{jp, lk} = \delta_{j, j \pm 1} \psi_{lk}^{j \pm}$, $\psi_B^{jp, j+1, k} = -(j+2)\psi^{jp, j+1, k}/2$, and $\psi_B^{jp, j-1, k} = (j-1)\psi^{jp, j-1, k}/2$ (see Ref. [25]) and defining

$$\begin{aligned} \partial_{\parallel}^{j+} &= \partial_{\parallel} - \frac{j+2}{2} \partial_{\parallel} \ln B, \\ \partial_{\parallel}^{j-} &= \partial_{\parallel} + \frac{j-1}{2} \partial_{\parallel} \ln B, \end{aligned} \quad (18)$$

we can combine the ψ and ψ_B terms to rewrite Eq. (12) as

$$\sum_k \psi_{pk}^{j-} \partial_{\parallel}^{j-} \hat{M}^{j-1, k} + \sum_k \psi_{pk}^{j+} \partial_{\parallel}^{j+} \hat{M}^{j+1, k} = \frac{1}{\lambda_C} \sum_k c_{pk}^j \hat{M}^{jk} + \frac{\partial_{\parallel} \ln B}{B/B_0} \left(g_p^{jp} \hat{p}_{\psi} + g_T^{jp} \hat{T}_{\psi} \right). \quad (19)$$

Although Eq. (12) for $j = 0, 1, \dots, L-1$ and $k = 0, 1, \dots, K-1$ is a truncated system, there exist L and K such that the solution does not change when increasing the number of moments higher than L and K . In other words, there exists a convergent solution of Eq. (12) which can be considered as a solution of Eq. (3). Therefore Eq. (12) for the truncated set of moments is quantitatively equivalent to Eq. (3).

III. FOURIER METHOD OF SOLVING MOMENT EQUATIONS

In the axisymmetric magnetic field (1), physical quantities on a flux surface depends on θ only. Using $\partial_{\parallel} = (\mathbf{B} \cdot \nabla \theta / B) \partial / \partial \theta = (B^{\theta} / B) \partial_{\theta}$ and dividing Eq. (12) by B^{θ} / B yields a system of ordinary differential equations

$$\sum_{lk} \psi^{jp, lk} \partial_{\theta} \hat{M}^{lk} + \psi_B^{jp, lk} (\partial_{\theta} \ln B) \hat{M}^{lk} = \frac{B}{B^{\theta} \lambda_C} c^{jp, lk} \hat{M}^{lk} + \frac{\partial_{\theta} \ln B}{B/B_0} \left(g_p^{jp} \hat{p}_{\psi} + g_t^{jp} \hat{T}_{\psi} \right). \quad (20)$$

Since the coefficient $\partial_\theta \ln B$ is θ -dependent, the eigenvector method used in deriving integral closures [30] does not work. Instead, we adopt the Fourier method to convert the system of differential equations to a system of algebraic equations. Note that Eq. (20) forms a linear system of ordinary differential equations for the parallel moments \hat{M}^{lk} and the Fourier expansion of coefficients, moments, and drive terms will convert the differential system to a linear algebraic system.

In the Fourier method, all physical quantities are expanded in Fourier series. For $A = \hat{M}^{lk}(\theta)$ and $\partial_\theta \ln B/(B/B_0)$,

$$A(\theta) = A_{(0)} + A_{(1-)} \sin \theta + A_{(1+)} \cos \theta + A_{(2-)} \sin 2\theta + A_{(2+)} \cos 2\theta + \dots = \sum_m A_{(m)} \varphi_{(m)}, \quad (21)$$

with Fourier modes

$$\begin{aligned} \varphi_{(0)} &= 1, \quad \varphi_{(1)} = \varphi_{(1-)} = \sin \theta, \quad \varphi_{(2)} = \varphi_{(1+)} = \cos \theta, \dots, \\ \varphi_{(2n-1)} &= \varphi_{(n-)} = \sin n\theta, \quad \varphi_{(2n)} = \varphi_{(n+)} = \cos n\theta, \dots \end{aligned} \quad (22)$$

where the Fourier index is denoted in the parentheses. The Fourier coefficient for $A(\theta)$ can be obtained by

$$A_{(m)} = \frac{1}{\sigma_{(m)}} \int d\theta \varphi_{(m)} A(\theta), \quad (23)$$

where $\sigma_{(0)} = 2\pi$ and $\sigma_{(m)} = \pi$ for $m > 0$. The derivative ∂_θ and the θ -dependent coefficients in Eq. (20) become matrices in Fourier representation. For $O = \partial_\theta$, $\partial_\theta \ln B$, and $B/B^\theta \lambda_C$, the Fourier matrix elements $O_{(i,j)}$ are obtained by

$$O_{(i,j)} = \frac{1}{\sigma_{(i)}} \int d\theta \varphi_{(i)} O \varphi_{(j)}, \quad (24)$$

and the Fourier representation of $O \hat{M}^{lk}$ becomes

$$\left(O \hat{M}^{lk} \right)_{(i)} = \frac{1}{\sigma_{(i)}} \int d\theta \varphi_{(i)} O \sum_j \hat{M}_{(j)}^{lk} \varphi_{(j)} = \sum_j O_{(i,j)} \hat{M}_{(j)}^{lk}. \quad (25)$$

Then the (m) th Fourier component of Eq. (20) becomes a system of algebraic equations

$$\begin{aligned} \psi^{jp, lk} (\partial_\theta)_{(m,n)} \hat{M}_{(n)}^{lk} + \psi_B^{jp, lk} (\partial_\theta \ln B)_{(m,n)} \hat{M}_{(n)}^{lk} = \\ c^{jp, lk} \left(\frac{B}{B^\theta \lambda_C} \right)_{(m,n)} \hat{M}_{(n)}^{lk} + \left(\frac{\partial_\theta \ln B}{B/B_0} \right)_{(m)} \left(g_p^{jp} \hat{p}_{0,\psi} + g_T^{jp} \hat{T}_{0,\psi} \right), \end{aligned} \quad (26)$$

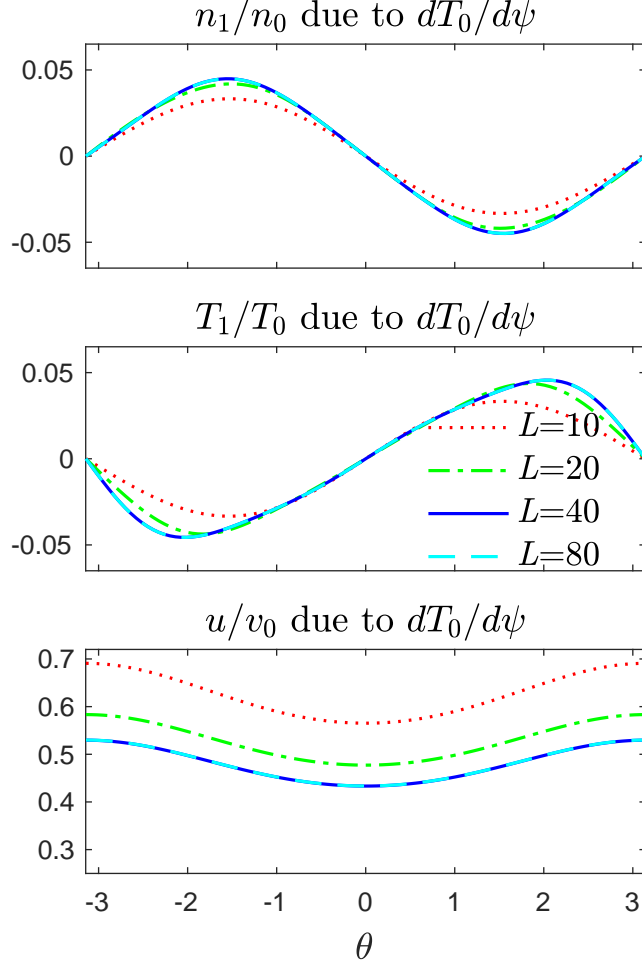


Figure 1. First-order density, temperature, and parallel flow velocity for $\epsilon = 0.1$, $K_0 = 100$, $\mathbf{n}_F = 4$, and for $LK = 10 \times 20$ (red, dotted), 20×40 (green, dash-dotted), 40×80 (blue solid), and 80×160 (cyan, dashed). The ratios n_1/n_0 , T_1/T_0 , and u/v_0 are plotted in units of $\hat{T}_{0,\psi}$.

where summation over l, k , and n is implied. The system of algebraic equations can be written in matrix form,

$$\llbracket \psi \partial_\theta \rrbracket \llbracket \hat{M} \rrbracket + \llbracket \psi_B \partial_\theta \ln B \rrbracket \llbracket \hat{M} \rrbracket = \llbracket cB/B^\theta \lambda_C \rrbracket \llbracket \hat{M} \rrbracket + \llbracket (g_p \hat{p}_0 + g_T \hat{T}_0)(B_0/B)(\partial_\theta \ln B) \rrbracket, \quad (27)$$

where $\llbracket \psi \partial_\theta \rrbracket = [\psi] \otimes (\partial_\theta)_F$, $\llbracket \psi_B \partial_\theta \ln B \rrbracket = [\psi_B] \otimes (\partial_\theta \ln B)_F$, and $\llbracket cB/B^\theta \lambda_C \rrbracket = [c] \otimes (B/B^\theta \lambda_C)_F$ with \otimes denoting a tensor product of two matrices. The i th row and j th column of a Fourier matrix $(O)_F$ is $O_{(i,j)}$, and the dimension of the linear system is $N = LKF =$ (the number of Legendre polynomials)(the number of Laguerre polynomials)(the number of Fourier modes).

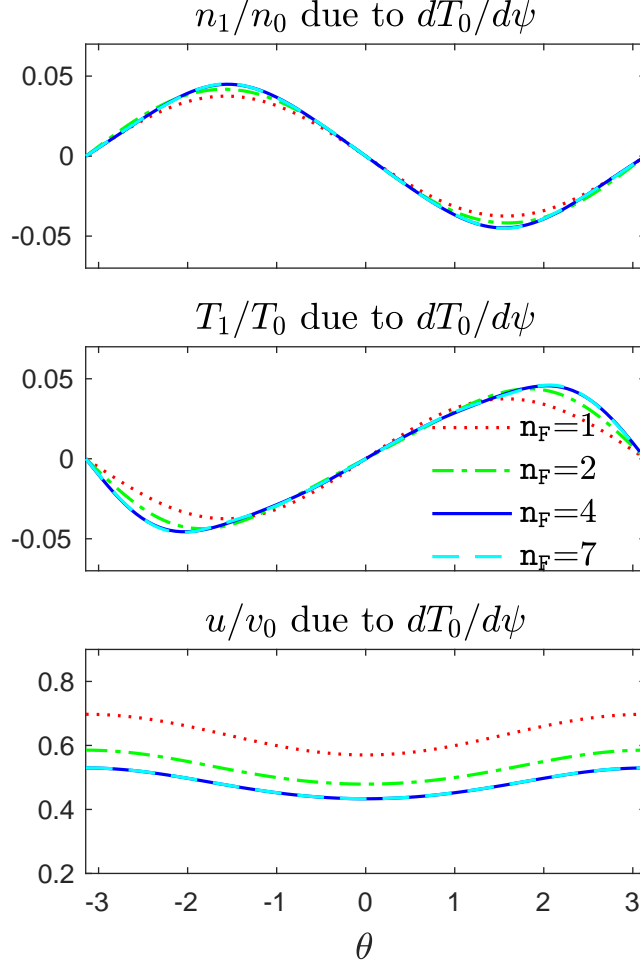


Figure 2. First-order density, temperature, and parallel flow velocity for $\epsilon = 0.1$, $K_0 = 100$, $LK = 40 \times 80$, and for $\mathbf{n}_F = 1$ (red, dotted), 2 (green, dash-dotted), 4 (blue solid), and 7 (cyan, dashed). The ratios n_1/n_0 , T_1/T_0 , and u/v_0 are plotted in units of $\hat{T}_{0,\psi}$.

The solution $\llbracket \hat{M} \rrbracket$ can be obtained by inverting or singular-value-decomposing the matrix,

$$\llbracket \hat{M} \rrbracket = \left(\llbracket \psi \partial_\theta \rrbracket + \llbracket \psi_B \partial_\theta \ln B \rrbracket - \llbracket cB/B^\theta \lambda_C \rrbracket \right)_{\text{ns}}^{-1} \llbracket (g_p \hat{p}_{0,\psi} + g_T \hat{T}_{0,\psi})(B_0/B)(\partial_\theta \ln B) \rrbracket, \quad (28)$$

where the subscript ‘ns’ denotes the nonsingular part of the matrix. It is found that eliminating $n_{(0)}$ and $T_{(0)}$ components makes the matrix nonsingular [see also remarks in relation to Eqs. (48) and (50)]. Then the Fourier components of the first order fluid quantities can

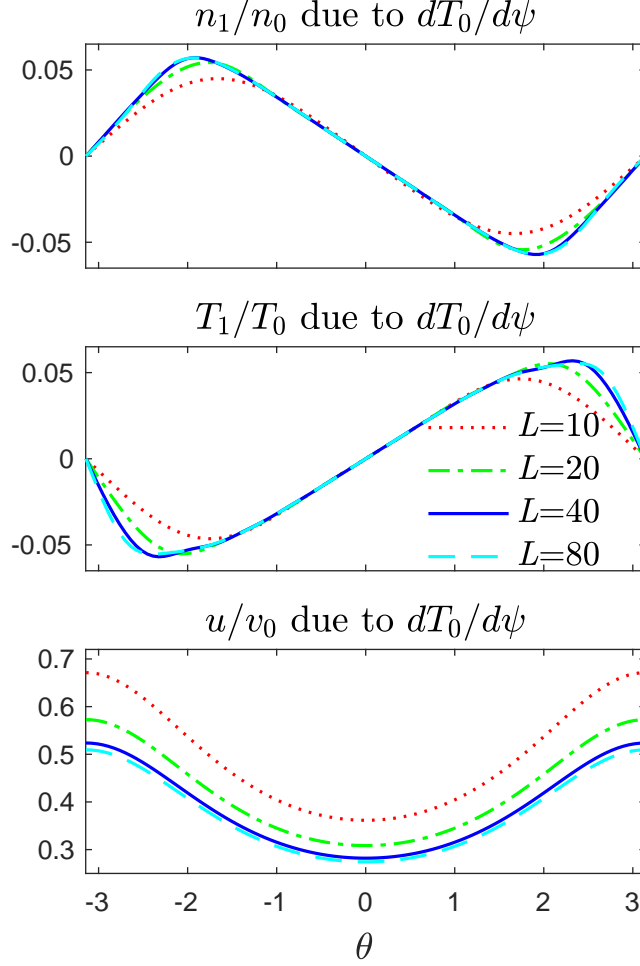


Figure 3. First-order density, temperature, and parallel flow velocity for $\epsilon = 0.3$, $K_0 = 100$, $\mathbf{n}_F = 4$, and for $LK = 10 \times 20$ (red, dotted), 20×40 (green, dash-dotted), 40×80 (blue solid), and 80×160 (cyan, dashed).

be read from the solution $\llbracket \hat{M} \rrbracket$,

$$\begin{aligned}
\mathbb{N} &= \hat{p}_{0,\psi} \mathbb{N}^{p_0} + \hat{T}_{0,\psi} \mathbb{N}^{T_0}, \\
\mathbb{T} &= \hat{p}_{0,\psi} \mathbb{T}^{p_0} + \hat{T}_{0,\psi} \mathbb{T}^{T_0}, \\
\mathbb{U} &= \hat{p}_{0,\psi} \mathbb{U}^{p_0} + \hat{T}_{0,\psi} \mathbb{U}^{T_0},
\end{aligned} \tag{29}$$

where $\mathbb{N} = (\hat{n})_F = (n_1/n_0)_F$, $\mathbb{T} = (\hat{T})_F = (T_1/T_0)_F$, $\mathbb{U} = (\hat{u})_F = (u/v_0)_F$, \mathbb{N}^α , \mathbb{T}^β , and \mathbb{U}^β ($\beta = p_0, T_0$) are column vectors of Fourier components. With the Fourier components, the first-order fluid quantities can be constructed from Eq. (21). For example, the density due to $\hat{p}_{0,\psi}$ and $\hat{T}_{0,\psi}$, respectively, are $\hat{n} = \sum_m \mathbb{N}_{(m)}^{p_0} \varphi_{(m)} \hat{p}_{0,\psi}$ and $\hat{n} = \sum_m \mathbb{N}_{(m)}^{T_0} \varphi_{(m)} \hat{T}_{0,\psi}$, where $\mathbb{N}_{(m)}^\beta$ is the (m) th Fourier component of the column vector \mathbb{N}^β .

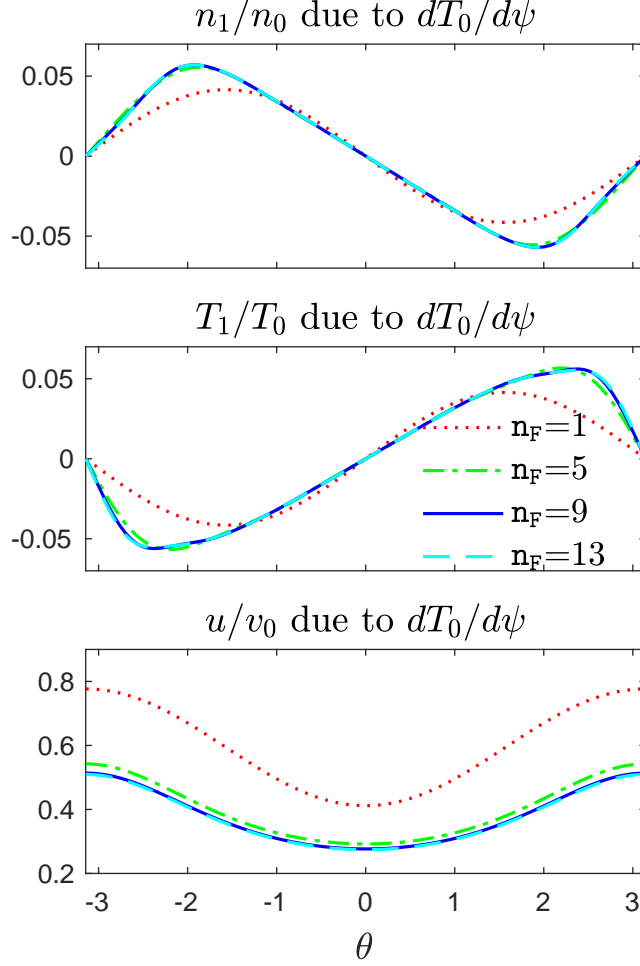


Figure 4. First-order density, temperature, and parallel flow velocity for $\epsilon = 0.3$, $K_0 = 100$, $N = LK = 40 \times 80$, and for $n_F = 1$ (red, dotted), 5 (green, dash-dotted), 9 (blue solid), and 13 (cyan, dashed). The ratios n_1/n_0 , T_1/T_0 , and u/v_0 are plotted in units of $\hat{T}_{0,\psi}$.

The inverse collisionality of the system is characterized by a Knudsen number, the ratio of the mean free path to the gradient scale length. Defining a basic Knudsen number for a tokamak $K_0 = B/B^\theta \lambda_C$, the effective Knudsen number would be roughly $K_0 \partial_\theta \ln B \sim m K_0$ where m is the typical Fourier mode of the system. Although the solution (28) can be obtained for an arbitrary axisymmetric magnetic field, circular magnetic fields [see Eq. (2)] are considered in this work. For the circular magnetic field (2), the basic Knudsen number is given by $K_0 \sim \lambda_C/qR_0$ where q is the safety factor and the Fourier mode m is determined by the inverse aspect ratio $\epsilon = r/R_0$. In general, the effective Knudsen number increases as λ_C and ϵ increase.

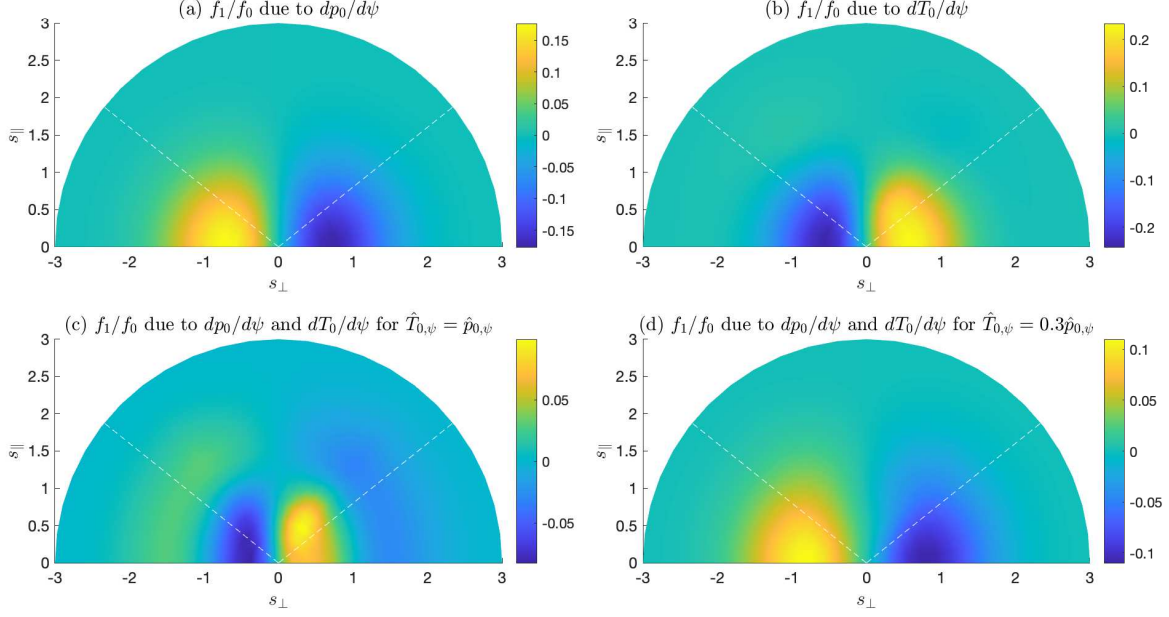


Figure 5. The first-order distribution function f_1 at $\theta = -\pi/3$ in the s_\perp - s_\parallel plane for $\epsilon = 0.3$ and $K_0 = 100$. The white dashed lines indicate the passing/trapped boundary. The ratio f_1/f_0 is plotted in units of $\hat{p}_{0,\psi}$ in (a), (c), and (d) and in units of $\hat{T}_{0,\psi}$ in (b).

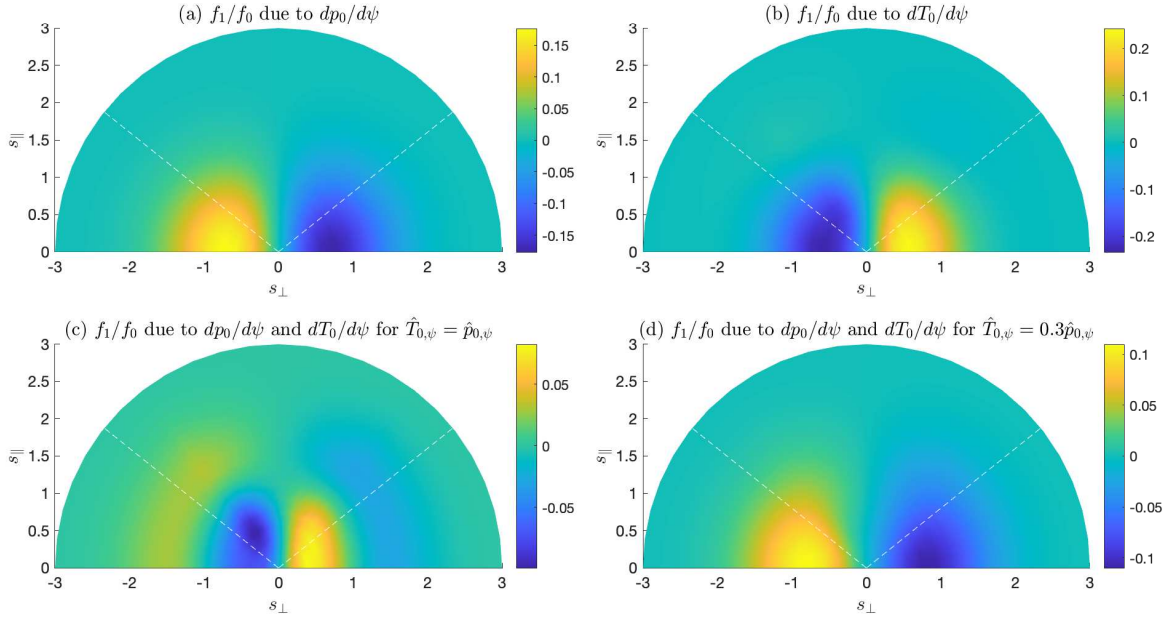


Figure 6. The first-order distribution function f_1 at $\theta = \pi/3$ on the s_\perp - s_\parallel plane for $\epsilon = 0.3$ and $K_0 = 100$. The white dashed lines indicate the passing/trapped boundary. The ratio f_1/f_0 is plotted in units of $\hat{p}_{0,\psi}$ in (a), (c), and (d) and in units of $\hat{T}_{0,\psi}$ in (b).

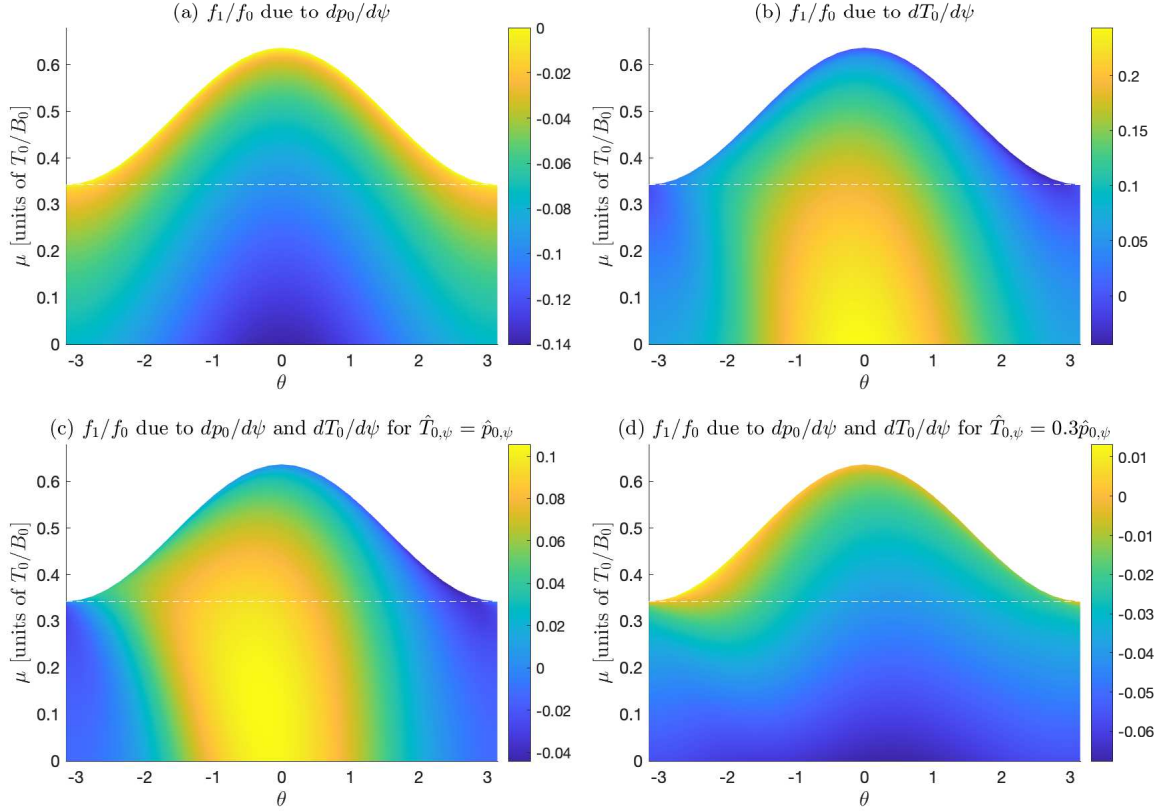


Figure 7. The first-order distribution function f_1 at $s = 0.7$ on the θ - μ plane for $\epsilon = 0.3$ and $K_0 = 100$. The white dashed line indicates the passing/trapped boundary. The ratio f_1/f_0 is plotted in units of $\hat{p}_{0,\psi}$ in (a), (c), and (d) and in units of $\hat{T}_{0,\psi}$ in (b).

The solution responding to the radial pressure gradient $dp_0/d\psi$ shows that $N^{p_0} = 0$, $T^{p_0} = 0$, and $U^{p_0} = -(1, 0, \epsilon, \dots)^T = -(B_0/B)_F$. This means that the $\hat{p}_{0,\psi}$ drive contributes only to the flow velocity as $\hat{u} = -\hat{p}_{0,\psi}B_0/B + \gamma^u B/B_0$, consistent with the continuity equation $\nabla \cdot (n_0 \mathbf{V}_1) = 0$. Here γ^u is an integration constant that can be determined by temperature and flow velocity equations. It turns out that γ^u is proportional to $\hat{T}_{0,\psi}$ as verified from the solution and as discussed in Sec. IV.

For the solution responding to the radial temperature gradient $dT_0/d\psi$, the density, temperature, and parallel flow velocity are shown in Fig. 1 in the case of $\epsilon = 0.1$, $K_0 = 100$, and $n_F = 4$ ($F = 2n_F + 1 = 9$). A convergence study increases the number of moments to show that the $LK = 40 \times 80$ moment solution converges and can be considered practically exact. Note that the polynomials \hat{P}^{lk} in Eq. (7) form a complete set. The necessary number of moments for convergence increases as K_0 increases. A convergence study that increases the

number of Fourier modes from 1 to 7 (see Figure 2) shows that the $\mathbf{n}_F = 4$ mode solution converges and may be considered to be very accurate. The necessary number of Fourier modes for convergence increases as ϵ increases.

Figures 3 and 4 show the density, temperature, and parallel flow velocity for $\epsilon = 0.3$, a larger inverse aspect ratio, and $K_0 = 100$. The $LK = 40 \times 80$ moment solution, while not as accurate as in the $\epsilon = 0.1$ case, is still very accurate for practical use, and the $LK = 80 \times 160$ solution is expected to be accurate. This is because $\epsilon = 0.3$ requires more Fourier modes than $\epsilon = 0.1$ for an accurate expansion of the magnetic field. Higher Fourier modes make the effective Knudsen number larger. The necessary number of Fourier modes for convergence is $\mathbf{n}_F = 13$.

The moment solution can be used to construct the distribution function that is a solution of the kinetic equation (3). Since all fluid quantities relevant to physical observables involve several lowest order of moments, the reconstruction of the distribution function from the moments may be redundant. Nevertheless, the distribution function itself is important for understanding the kinetic behavior of a plasma. In the moment expansion, the high order moments near truncation of the moment expansion could be inaccurate and may adversely affect the convergence of the distribution function. However we find that those moments near truncation are several orders smaller than the fluid moments, making the truncation errors ignorable once the convergence is achieved. Figures 5 and 6 show the distribution functions constructed from the moment solution on the s_\perp - s_\parallel plane at $\theta = -\pi/3$ and $\pi/3$, respectively. Figure 7 shows the distribution function at $s = 0.7$ on the θ - μ plane.

IV. FLUID EQUATIONS AND CLOSURES

In neoclassical transport theory, one solves Eq. (3) to express f_1 in terms of f_0 (or F) and take moments of the solution f_1 to express u in terms of $dp_0/d\psi$ and $dT_0/d\psi$. These expressions can be directly obtained by solving Eq. (12). In this section we derive closure relations that can be used for closing and advancing (nonlinear) fluid equations for density, flow velocity, and temperature. They can also be incorporated into linearized fluid equations to reproduce the expressions of n_1 , T_1 and u that are obtained in Sec. III. Although the closures

are represented in the Fourier basis, the formalism developed here can be applied to any basis such as a finite element basis or finite difference basis in numerical methods.

The linearized fluid equations for n_1 , u , and T_1 can be obtained from the original fluid equations with $n = n_0 + n_1$, $T = T_0 + T_1$, $\mathbf{V} = u\mathbf{b} + \mathbf{b} \times \nabla p_0/n_0 qB$, $\mathbf{h} = h_{\parallel}\mathbf{b} + 5p_0\mathbf{b} \times \nabla T_0/2qB$, and $\boldsymbol{\pi} = (3\pi_{\parallel}/2)(\mathbf{b}\mathbf{b} - b^2\mathbf{I}/3)$ where $\mathbf{b} = \mathbf{B}/B$. They are equivalent to the $\{P^{00}, mv_0 P^{10}, -T_0 P^{01}\}$ moments of Eq. (3) and can be read from Eq. (20) for $(j, p) = (0, 0)$, $(1, 0)$, and $(0, 1)$:

$$\partial_{\theta}^{0+}\hat{u} = 2\hat{p}_{0,\psi} \frac{\partial_{\theta} \ln B}{B/B_0}, \quad (30)$$

$$\partial_{\theta}^{0+}\hat{u} + \partial_{\theta}^{0+}\hat{h} = (2\hat{p}_{0,\psi} + 5\hat{T}_{0,\psi}) \frac{\partial_{\theta} \ln B}{B/B_0}, \quad (31)$$

$$\partial_{\theta}^{1-}\hat{n} + \partial_{\theta}^{1-}\hat{T} + \partial_{\theta}^{1+}\hat{\pi} = 0, \quad (32)$$

where $\hat{u} = u/v_0$, $\hat{h} = h_{\parallel}/v_0 p_0$, $\hat{\pi} = \pi_{\parallel}/p_0$, and $\partial_{\theta}^{l\pm}$ is defined by Eq. (18) with ∂_{\parallel} replaced by ∂_{θ} . For this fluid system to be closed, closure quantities \hat{h} and $\hat{\pi}$ should relate to first-order (\hat{n} , \hat{u} , and \hat{T}) and equilibrium ($\hat{p}_{0,\psi}$ and $\hat{T}_{0,\psi}$) fluid quantities.

In order to obtain the closure relations, the rows corresponding to fluid equations need to be removed from Eq. (20). Then the corresponding columns appear as drives (sources) $[g_{\theta}]$ in the system:

$$[\psi'] \left[\partial_{\theta} \hat{M}' \right] + [\psi'_B] (\partial_{\theta} \ln B) \left[\hat{M}' \right] = \frac{B}{B^{\theta} \lambda_C} [c'] \left[\hat{M}' \right] + [g_{\theta}] + \frac{\partial_{\theta} \ln B}{B/B_0} \left([g'_p] \hat{p}_{0,\psi} + [g'_T] \hat{T}_{0,\psi} \right), \quad (33)$$

where \prime denotes the removal of fluid columns and rows. For example, $\left[\hat{M}' \right]$ is a column vector $(\hat{M}^{0,2}, \dots, \hat{M}^{0,K+1}, \hat{M}^{1,1}, \dots, \hat{M}^{1,K}, \hat{M}^{2,0}, \dots, \hat{M}^{2,K-1}, \dots, \hat{M}^{L-1,0}, \dots, \hat{M}^{L-1,K-1})$. The nonvanishing elements of $[g_{\theta}]$ are

$$g_{\theta}^{1,1} = \frac{\sqrt{5}}{2} \partial_{\theta} \hat{T}, \quad (34)$$

$$g_{\theta}^{2,0} = -\frac{\sqrt{3}}{2} W_{\theta}, \quad W_{\theta} = \frac{4}{3} \partial_{\parallel}^{2-} \hat{u}. \quad (35)$$

From Fourier representation of Eq. (33),

$$\llbracket \psi' \partial_{\theta} \rrbracket \llbracket \hat{M}' \rrbracket + \llbracket \psi'_B \partial_{\theta} \ln B \rrbracket \llbracket \hat{M}' \rrbracket = \llbracket cB/B^{\theta} \lambda_C \rrbracket \llbracket \hat{M}' \rrbracket + \llbracket g_{\theta} \rrbracket + \llbracket (g'_p \hat{p}_0 + g'_T \hat{T}_0)(B_0/B)(\partial_{\theta} \ln B) \rrbracket,$$

(36)

the solution can be obtained,

$$\llbracket \hat{M}' \rrbracket = (\llbracket \psi' \partial_\theta \rrbracket + \llbracket \psi'_B \partial_\theta \ln B \rrbracket - \llbracket cB/B^\theta \lambda_C \rrbracket)^{-1} \llbracket g_\theta + (g_p \hat{p}_{0,\psi} + g_T \hat{T}_{0,\psi})(B_0/B)(\partial_\parallel \ln B) \rrbracket. \quad (37)$$

Fourier components of closures $\hat{h} = -\sqrt{5}\hat{M}^{1,1}/2$ and $\hat{\pi} = 2\hat{M}^{2,0}/\sqrt{3}$ can be read from the solution and expressed in terms of $\hat{p}_{0,\psi}$, and $\hat{T}_{0,\psi}$, \hat{T} , and \hat{u} :

$$\mathbb{H} = \hat{p}_{0,\psi} \mathbb{H}^{p_0} + \hat{T}_{0,\psi} \mathbb{H}^{T_0} + \mathbf{K}^{hh} \mathbf{D} \mathbb{T} + \mathbf{K}^{h\pi} \mathbb{W}, \quad (38)$$

$$\mathbb{S} = \hat{p}_{0,\psi} \mathbb{S}^{p_0} + \hat{T}_{0,\psi} \mathbb{S}^{T_0} + \mathbf{K}^{\pi h} \mathbf{D} \mathbb{T} + \mathbf{K}^{\pi\pi} \mathbb{W}, \quad (39)$$

where $\mathbb{H} = (\hat{h})_{\mathbf{F}}$, $\mathbb{S} = (\hat{\pi})_{\mathbf{F}}$, and $\mathbb{W} = (W_\theta)_{\mathbf{F}} = (4/3)\mathbf{D}^{2-}\mathbb{U} \equiv \mathbf{D}_W \mathbb{U}$, \mathbb{H}^β , and \mathbb{S}^β ($\beta = p_0, T_0$) are column vectors, and $\mathbf{D} = (\partial_\theta)_{\mathbf{F}}$, $\mathbf{D}^{l\pm} = (\partial_\theta^{l\pm})_{\mathbf{F}}$, and $\mathbf{K}^{\alpha\beta}$ ($\alpha, \beta = h, \pi$) are matrices. Here a column vector \mathbb{H}^β and \mathbb{S}^β connects the closures h_\parallel and π_\parallel to a radial gradient of zeroth-order pressure ($\beta = p_0$) or temperature ($\beta = T_0$), and a matrix $\mathbf{K}^{\alpha\beta}$ connects closures $\alpha = h$ and π to a parallel gradient of first-order temperature ($\beta = h$) or parallel flow velocity ($\beta = \pi$). The closures in the position space can be constructed from the solution vector, for example, $\hat{h}(\theta) = \sum_i \varphi_{(i)} \{ \mathbb{H}_{(i)}^{p_0} \hat{p}_{0,\psi} + \mathbb{H}_{(i)}^{T_0} \hat{T}_{0,\psi} + \sum_j [\mathbf{K}_{(i,j)}^{hh} (\mathbf{D} \mathbb{T})_{(j)} + \mathbf{K}_{(i,j)}^{h\pi} \mathbb{W}_{(j)}] \varphi_{(j)} \}$, where $\mathbb{H}_{(i)}^\beta$ is the (i) th Fourier component of the column vector \mathbb{H}^β and $\mathbf{K}_{(i,j)}^{\alpha\beta}$ is the (i) th row and (j) th column of the matrix $\mathbf{K}^{\alpha\beta}$. Figures 8 and 9, respectively, show the parallel heat flux density and viscosity due to $\hat{p}_{0,\psi}$, $\hat{T}_{0,\psi}$, and several Fourier modes of $\partial_\theta \hat{T}$ and W_θ . As the Fourier mode of the thermodynamic drives increases, the contribution to the closure quantity decreases.

By combining closure relations with the time-independent, linear fluid equations, we can reproduce the fluid variables of Sec. III. Using $(B_0/B)\partial_\theta \ln B = -\partial_\theta(B_0/B)$ and eliminating Eq. (30) from Eq. (31), we write the Fourier representation of Eqs. (30)-(32),

$$\mathbf{D}^{0+} \mathbb{U} = -2\hat{p}_{0,\psi} \mathbf{D} \mathbb{B}_{-1}, \quad (40)$$

$$\mathbf{D}^{0+} \mathbb{H} = -5\hat{T}_{0,\psi} \mathbf{D} \mathbb{B}_{-1}, \quad (41)$$

$$\mathbf{D} \mathbb{N} + \mathbf{D} \mathbb{T} + \mathbf{D}^{1+} \mathbb{S} = 0, \quad (42)$$

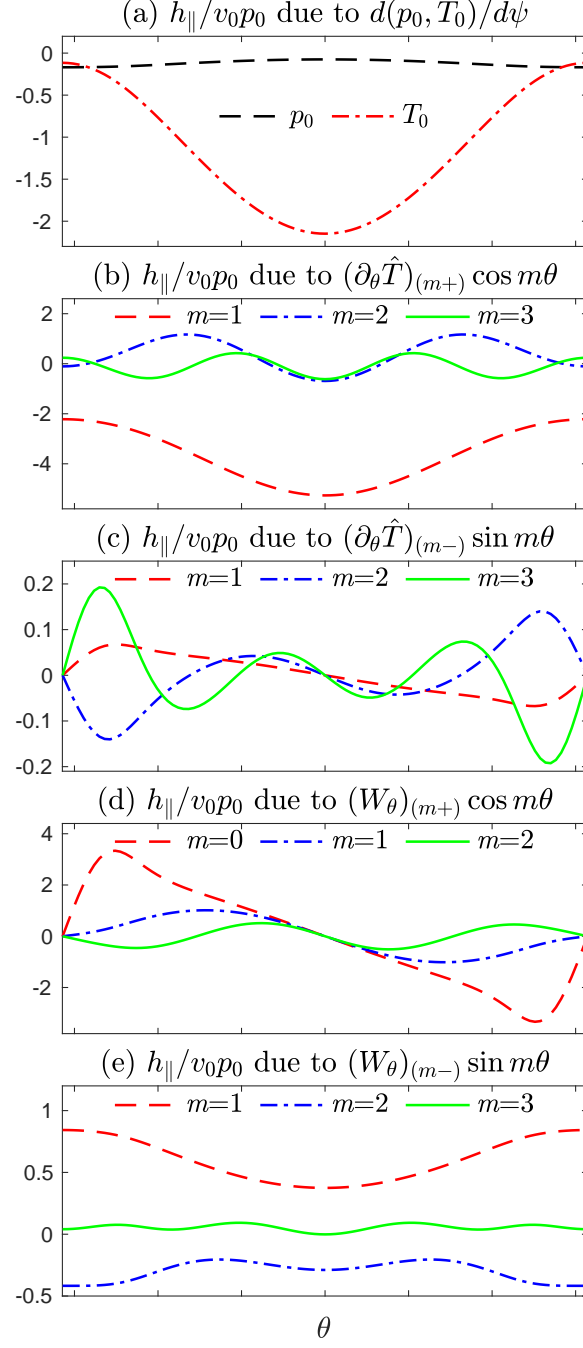


Figure 8. Parallel heat flux density due to (a) $dp_0/d\psi$ and $dT_0/d\psi$, (b) $(\partial_\theta \hat{T})_{(m+)} \cos m\theta$, (c) $(\partial_\theta \hat{T})_{(m-)} \sin m\theta$, (d) $(W_\theta)_{(m+)} \cos m\theta$, and (e) $(W_\theta)_{(m-)} \sin m\theta$. The dimensionless heat flux, $h_\parallel/v_0 p_0$, is plotted in units of (a) $\hat{p}_{0,\psi}$ and $\hat{T}_{0,\psi}$, (b) $(\partial_\theta \hat{T})_{(m+)}$, (c) $(\partial_\theta \hat{T})_{(m-)}$, (d) $(W_\theta)_{(m+)}$, and (e) $(W_\theta)_{(m-)}$.

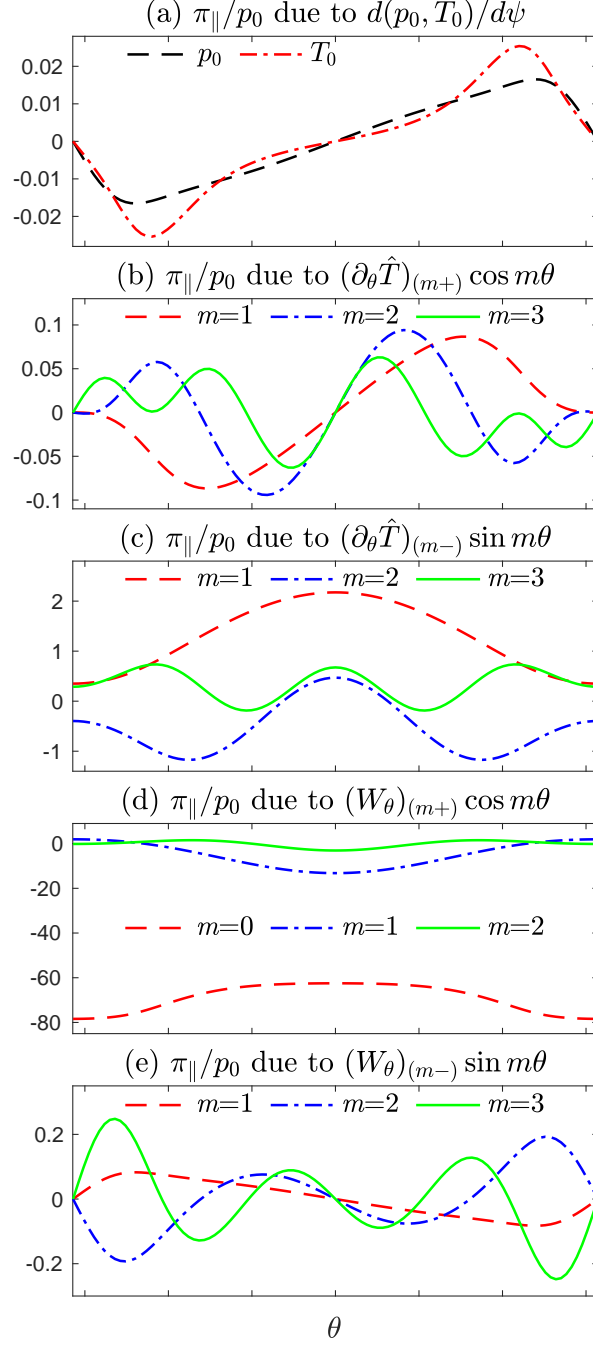


Figure 9. Parallel viscosity due to (a) $dp_0/d\psi$ and $dT_0/d\psi$, (b) $(\partial_{\theta}\hat{T})_{(m+)} \cos m\theta$, (c) $(\partial_{\theta}\hat{T})_{(m-)} \sin m\theta$, (d) $(W_{\theta})_{(m+)} \cos m\theta$, and (e) $(W_{\theta})_{(m-)} \sin m\theta$. The dimensionless viscosity π_{\parallel}/p_0 is plotted in units of (a) $\hat{p}_{0,\psi}$ and $\hat{T}_{0,\psi}$, (b) $(\partial_{\theta}\hat{T})_{(m+)}$, (c) $(\partial_{\theta}\hat{T})_{(m-)}$, (d) $(W_{\theta})_{(m+)}$, and (e) $(W_{\theta})_{(m-)}$.

where $\mathbb{B}_{-1} = (B_0/B)_{\text{F}}$. Then we combine with closures (38) and (39) to write

$$\mathbf{L} \begin{pmatrix} \mathbb{N} \\ \mathbb{T} \\ \mathbb{U} \end{pmatrix} = \mathbb{R}^{p_0} \hat{p}_{0,\psi} + \mathbb{R}^{T_0} \hat{T}_{0,\psi}. \quad (43)$$

where

$$\mathbf{L} = \begin{pmatrix} 0 & 0 & \mathbf{D}^{0+} \\ 0 & \mathbf{D}^{0+} \mathbf{K}^{hh} \mathbf{D} & \mathbf{D}^{0+} \mathbf{K}^{h\pi} \mathbf{D}_W \\ \mathbf{D} & \mathbf{D} + \mathbf{D}^{1+} \mathbf{K}^{\pi h} \mathbf{D} & \mathbf{D}^{1+} \mathbf{K}^{\pi\pi} \mathbf{D}_W \end{pmatrix}, \quad (44)$$

$$\mathbb{R}^{p_0} = - \begin{pmatrix} 2\mathbf{D}\mathbb{B}^{-1} \\ \mathbf{D}^{0+} \mathbb{H}^{p_0} \\ \mathbf{D}^{1+} \mathbb{S}^{p_0} \end{pmatrix}, \quad \mathbb{R}^{T_0} = - \begin{pmatrix} 0 \\ 5\mathbf{D}\mathbb{B}^{-1} \\ \mathbf{D}^{1+} \mathbb{S}^{T_0} \end{pmatrix}. \quad (45)$$

Using the singular value decomposition, we can invert the nonsingular part of \mathbf{L} and obtain the solution vector $(\mathbb{N}, \mathbb{T}, \mathbb{U})$ in terms of $\hat{p}_{0,\psi}$ and $\hat{T}_{0,\psi}$. The solution vector reproduces Eq. (29) with the column vector $(\mathbb{N}^\beta, \mathbb{T}^\beta, \mathbb{U}^\beta) = (\mathbf{L}_{\text{ns}}^{-1}) \mathbb{R}^\beta$ for $\beta = p_0$ and T_0 .

Now we discuss how to obtain the parallel flow velocity and heat flux density when not using the singular value decomposition but instead, analytically calculating the integration constants. From Eqs. (40) and (41), we have

$$\mathbb{U} = -\hat{p}_{0,\psi} \mathbb{B}_{-1} + \gamma^u \mathbb{B}, \quad (46)$$

$$\mathbb{H} = -\frac{5}{2} \hat{T}_{0,\psi} \mathbb{B}_{-1} + \gamma^h \mathbb{B}, \quad (47)$$

where γ^u and γ^h are expansion coefficients for the null space of \mathbf{D}^{0+} ($\mathbf{D}^{0+} \mathbb{B} = 0$), and $\mathbb{B} = (B/B_0)_{\text{F}}$. Combining Eq. (38) with (47), we have

$$\mathbf{D}\mathbb{T} = \gamma^u \mathbb{F}^u + \gamma^h \mathbb{F}^h + \hat{p}_{0,\psi} \mathbb{F}^p + \hat{T}_{0,\psi} \mathbb{F}^T, \quad (48)$$

where

$$\begin{aligned} \mathbb{F}^u &= -\mathbf{K}^{hh,-1} \mathbf{K}^{h\pi} \mathbf{D}_W \mathbb{B}, \\ \mathbb{F}^h &= \mathbf{K}^{hh,-1} \mathbb{B}, \\ \mathbb{F}^p &= -\mathbf{K}^{hh,-1} (\mathbb{H}^{p_0} - \mathbf{K}^{h\pi} \mathbf{D}_W \mathbb{B}_{-1}), \\ \mathbb{F}^T &= -\mathbf{K}^{hh,-1} \left(\mathbb{H}^{T_0} + \frac{5}{2} \mathbb{B}_{-1} \right), \end{aligned} \quad (49)$$

Combining Eq. (39) with Eq. (42) and using Eqs. (46) and (48), we have

$$\mathbf{D}\mathbf{N} + \mathbf{D}\mathbf{T} = \gamma^u \mathbb{G}^u + \gamma^h \mathbb{G}^h + \hat{p}_{0,\psi} \mathbb{G}^p + \hat{T}_{0,\psi} \mathbb{G}^T \quad (50)$$

where

$$\begin{aligned} \mathbb{G}^u &= -\mathbf{D}^{1+} \left(\mathbf{K}^{\pi h} \mathbb{F}^u + \mathbf{K}^{\pi\pi} \mathbf{D}_W \mathbb{B} \right), \\ \mathbb{G}^h &= -\mathbf{D}^{1+} \mathbf{K}^{\pi h} \mathbb{F}^h, \\ \mathbb{G}^p &= -\mathbf{D}^{1+} \left(\mathbb{S}^{p_0} + \mathbf{K}^{\pi h} \mathbb{F}^p - \mathbf{K}^{\pi\pi} \mathbf{D}_W \mathbb{B}_{-1} \right), \\ \mathbb{G}^T &= -\mathbf{D}^{1+} \left(\mathbb{S}^{T_0} + \mathbf{K}^{\pi h} \mathbb{F}^T \right). \end{aligned} \quad (51)$$

The temperature and density can be obtained by inverting the nonsingular part of \mathbf{D} in Eqs. (48) and (50). The null space of \mathbf{D} is spanned by $[\varphi_{(0)}]_{\mathbb{F}}$, which corresponds to the constant term in the Fourier series. Since the lowest-order density (n_0) and temperature (T_0) are constant, we set $n_{(0)} = 0$ and $T_{(0)} = 0$ without loss of generality. From the first row corresponding to the constant (0) Fourier mode,

$$0 = \gamma^u \mathbb{F}_{(0)}^u + \gamma^h \mathbb{F}_{(0)}^h + \hat{p}_{0,\psi} \mathbb{F}_{(0)}^p + \hat{T}_{0,\psi} \mathbb{F}_{(0)}^T, \quad (52)$$

$$0 = \gamma^u \mathbb{G}_{(0)}^u + \gamma^h \mathbb{G}_{(0)}^h + \hat{p}_{0,\psi} \mathbb{G}_{(0)}^p + \hat{T}_{0,\psi} \mathbb{G}_{(0)}^T, \quad (53)$$

we can determine the integration constants γ^u and γ^h ,

$$\begin{pmatrix} \gamma^u \\ \gamma^h \end{pmatrix} = - \begin{pmatrix} \mathbb{F}_{(0)}^u & \mathbb{F}_{(0)}^h \\ \mathbb{G}_{(0)}^u & \mathbb{G}_{(0)}^h \end{pmatrix}^{-1} \begin{pmatrix} \mathbb{F}_{(0)}^p & \mathbb{F}_{(0)}^T \\ \mathbb{G}_{(0)}^p & \mathbb{G}_{(0)}^T \end{pmatrix} \begin{pmatrix} \hat{p}_{0,\psi} \\ \hat{T}_{0,\psi} \end{pmatrix}. \quad (54)$$

Then Eqs. (46) and (47) with the constants obtained in Eq. (54) agree with the corresponding column vectors of the solution (28). Note that the heat flux obtained here is not a closure and satisfies $\nabla \cdot \mathbf{h} = 0$.

Before concluding this section, a few remarks are in order. First, Eqs. (40) and (41) are equivalent to $\nabla \cdot (n_0 \mathbf{V}_1) = 0$ and $\nabla \cdot \mathbf{h} = 0$. Inserting the lowest order solutions $\mathbf{V}_{1\perp} = (1/qB^2) \mathbf{B} \times \nabla p_0$ and $\mathbf{h}_{\perp} = (5p_0/2qB^2) \mathbf{B} \times \nabla T_0$ obtained from $\nabla p_0 - n_0 q \mathbf{V}_1 \times \mathbf{B}/m = 0$ and $(5/2)p_0 \nabla T_0 - q \mathbf{h} \times \mathbf{B} = 0$, one can derive $\hat{u} = -\hat{p}_{0,\psi} B_0/B + \gamma^u B/B_0$ and $\hat{h} = -5\hat{T}_{0,\psi} B_0/2B + \gamma^h B/B_0$ where γ^u and γ^h are integration constants. Second, \mathbb{F}^p and \mathbb{G}^p vanish when ion-electron collisions are ignored. By setting $f_1 = g + F$, Eq. (3) becomes $v_{\parallel} \partial_{\parallel} g = C(g) + C(F)$. Note that the $\hat{p}_{0,\psi}$ term in $C(F) = C(F, f^0) + C(f^0, F)$ vanishes due

to momentum conservation and does not affect g . Therefore the term $\hat{p}_{0,\psi}$ contributes only to the flow velocity moment of f_1 and hence \mathbb{F}^p in Eq. (48) and \mathbb{G}^p in Eq. (50) must vanish. Third, in the closure calculation, the $\hat{p}_{0,\psi}$ drive appears in W_θ of the viscosity equation and affects closure quantities. However, the $\hat{p}_{0,\psi}$ term in $V_{1\parallel}$ of W_θ exactly cancels the $\hat{p}_{0,\psi}$ term in $\mathbf{V}_{1\perp}$ of W_θ making n_1 and T_1 independent of the $\hat{p}_{0,\psi}$ drive. Fourth, for an electron-ion plasma $(a, b) = (e, i)$ and (i, e) , the $\hat{p}_{a0,\psi}$ and $\hat{p}_{b0,\psi}$ drives do not vanish in the collision operator $C(F_a, f_b^0) + C(f_a^0, F_b)$ for the g_a equation and do affect g_a unless $V_{1a\parallel} = V_{1b\parallel}$.

V. CONCLUSION AND FUTURE WORK

We have demonstrated how to solve the drift kinetic equation using the general moment equations to obtain transport and closure relations. Using the moment-Fourier method developed here, one can directly solve a full set of parallel moment equations equivalent to the drift kinetic equation for fluid variables (density, flow velocity, and temperature) and/or fluxes (particle flux, electric current, heat flux, etc.). The solution moments can be used to construct the distribution function that is the solution of the drift kinetic equation. One can also solve the non-Maxwellian moment equations to express parallel closures in terms of fluid variables. The closures can be combined with linearized fluid equations to reproduce the fluid variables and/or fluxes obtained from the full set of parallel moment equations. More importantly, the closures can be utilized to advance a system of fluid equations in numerical simulations with nonlinear terms kept when nonlinear effects are significant. Note that the drift kinetic equation yields only linearized fluid equations by nature, e.g. Eqs. (30)-(32), and hence cannot capture the nonlinear effects.

While the formalism developed here is only applied in the case of a single component plasma in a circular axisymmetric magnetic field, it can be generalized to a multi-component plasma in a tokamak with arbitrarily shaped nested flux surfaces. As long as the magnetic field is Fourier-expandable, the moment-Fourier approach developed here is applicable. For a multi-component plasma, the collisional heating and friction terms, respectively, will modify Eqs. (31) and (32). The collision terms introduce couplings of temperatures and flow velocities between unlike species and, as a result, the $dp_0/d\psi$ term will affect all other fluid and closure moments as remarked at the end of Sec. IV. Although ion-electron collisions in the

ion theory are ignored based on the small-mass-ratio approximation in the existing theories (including this work), the momentum and energy conservations require those terms in the ion fluid equations. These effects can be investigated by solving coupled moment equations with the Fourier method. The transport and closure relations for an electron-ion plasma will be presented in the near future.

The moment-Fourier method developed here is applicable to a plasma with an arbitrary Knudsen number in a general magnetic field, as long as convergence can be achieved by increasing the number of moments and Fourier modes. In the high-collisionality limit, $B/B^\theta \lambda_C \ll 1$, the closure coefficients $K^{\alpha\beta}$ in Eqs. (38) and (39) reproduce the corresponding Braginskii closure coefficient [32, 33]. In the small inverse aspect ratio limit, $\epsilon \ll 1$, the $K^{\alpha\beta}$ reproduce the corresponding integral closure [31]. In principle, the moment-Fourier solutions are practically exact once convergence is achieved. The necessary numbers of moments and Fourier modes, respectively, increase as the Knudsen number and the inverse aspect ratio increase. In practice, the moment approach is limited by the accuracy of the inverse matrix in Eqs. (28) and (37). For low collisionality $n_F K_0 \gtrsim 10^4$, the required matrix dimension for convergence is $LKF \gtrsim 10^6$, and the inverse matrix becomes inaccurate due to a large condition number, even with the exact null space eliminated in the case of Eq. (28). For low collisionality, the drift kinetic equation may be solved numerically. However, in the collisionless limit, we find that the drift kinetic equation should be solved analytically for accurate closure and transport relations. The results in the collisionless limit will be presented in the near future, too. It is also notable that the finite element basis used in Refs. [18] and [19] makes the convergence faster than the Legendre polynomial basis.

Since the computational effort to calculate the convergent closures is tremendous when the effective collisionality is low, it may be impractical to compute the closures during a fluid simulation. For practical applications, we plan to develop explicit formulas of closures which can be expressed in terms of magnetic field parameters, ϵ for a circular geometry or Fourier components for a general magnetic field. The explicit expressions of closures can be developed for practical values of $\epsilon \lesssim 0.4$ (at the edge of the ITER tokamak) and $n_F K_0 \lesssim 10^4$ (at the core of ITER). Once the closures have been obtained for the magnetic field parameters, they can be conveniently used without time-consuming moment calculations. Furthermore, calculating γ^u in Eq. (46) will be performed for general ϵ and collisionality of

interest for a quantitative analysis of convergence depending on the number of moments and Fourier modes.

DATA AVAILABILITY STATEMENT

The data that support the findings of this study are available upon request from the authors.

ACKNOWLEDGMENTS

The research was supported by the U.S. DOE under Grant Nos. DE-SC0022048 and DE-FG02-04ER54746 and by National R&D Program through the National Research Foundation of Korea (NRF) funded by Ministry of Science and ICT (2021M3F7A1084419).

-
- [1] A. A. Galeev and R. Z. Sagdeev, Soviet Physics JETP **26**, 233 (1968).
 - [2] M. N. Rosenbluth, R. D. Hazeltine, and F. L. Hinton, Phys. Fluids **15**, 116 (1972).
 - [3] R. D. Hazeltine, F. L. Hinton, and M. N. Rosenbluth, The Physics of Fluids **16**, 1645 (1973), <https://aip.scitation.org/doi/pdf/10.1063/1.1694191>.
 - [4] F. L. Hinton and R. D. Hazeltine, Rev. Mod. Phys. **48**, 239 (1976).
 - [5] S. P. Hirshman and D. J. Sigmar, Nucl. Fusion **21**, 1079 (1981).
 - [6] C. S. Chang and F. L. Hinton, The Physics of Fluids **25**, 1493 (1982), <https://aip.scitation.org/doi/pdf/10.1063/1.863934>.
 - [7] M. Taguchi, Plasma Physics and Controlled Fusion **30**, 1897 (1988).
 - [8] R. D. Hazeltine, Plasma Phys. **15**, 77 (1973).
 - [9] R. D. Hazeltine and J. D. Meiss, *Plasma Confinement* (Dover Pub., Inc., New York, 2003).
 - [10] R. Balescu, *Transport Processes in Plasmas* (North-Holland, Amsterdam, 1988) vols. 1 and 2.
 - [11] P. Helander and D. J. Sigmar, *Collisional Transport in Magnetized Plasmas* (Cambridge University Press, Cambridge, 2002).
 - [12] E. A. Belli and J. Candy, Plasma Physics and Controlled Fusion **50**, 095010 (2008).

- [13] E. A. Belli and J. Candy, Plasma Physics and Controlled Fusion **51**, 075018 (2009).
- [14] E. A. Belli and J. Candy, Plasma Physics and Controlled Fusion **54**, 015015 (2011).
- [15] M. Landreman and D. R. Ernst, Plasma Physics and Controlled Fusion **54**, 115006 (2012).
- [16] M. Landreman and D. R. Ernst, Journal of Computational Physics **243**, 130 (2013).
- [17] E. D. Held, S. E. Kruger, J.-Y. Ji, E. A. Belli, and B. C. Lyons, Physics of Plasmas **22**, 032511 (2015), <https://doi.org/10.1063/1.4914165>.
- [18] J. R. Jepson, C. C. Hegna, E. D. Held, J. A. Spencer, and B. C. Lyons, Physics of Plasmas **28**, 082503 (2021), <https://doi.org/10.1063/5.0054978>.
- [19] J. A. Spencer, B. Adair, E. D. Held, J.-Y. Ji, and J. R. Jepson, Journal of Computational Physics **450**, 110862 (2022).
- [20] C. Sovinec, A. Glasser, T. Gianakon, D. Barnes, R. Nebel, S. Kruger, D. Schnack, S. Plimpton, A. Tarditi, and M. Chu, Journal of Computational Physics **195**, 355 (2004).
- [21] S. C. Jardin, N. Ferraro, X. Luo, J. Chen, J. Breslau, K. E. Jansen, and M. S. Shephard, Journal of Physics: Conference Series **125**, 012044 (2008).
- [22] J. Breslau, N. Ferraro, and S. Jardin, Physics of Plasmas **16**, 092503 (2009), <https://doi.org/10.1063/1.3224035>.
- [23] B. Dudson, M. Umansky, X. Xu, P. Snyder, and H. Wilson, Computer Physics Communications **180**, 1467 (2009).
- [24] M. Hoelzl, G. Huijsmans, S. Pamela, M. Bécoulet, E. Nardon, F. Artola, B. Nkonga, C. Atanasiu, V. Bandaru, A. Bhole, D. Bonfiglio, A. Cathey, O. Czarny, A. Dvornova, T. Fehér, A. Fil, E. Franck, S. Futatani, M. Gruca, H. Guillard, J. Haverkort, I. Holod, D. Hu, S. Kim, S. Korving, L. Kos, I. Krebs, L. Kripner, G. Latu, F. Liu, P. Merkel, D. Meshcheriakov, V. Mitterauer, S. Mochalsky, J. Morales, R. Nies, N. Nikulsin, F. Orain, J. Pratt, R. Ramasamy, P. Ramet, C. Reux, K. Särkimäki, N. Schwarz, P. S. Verma, S. Smith, C. Sommariva, E. Strumberger, D. van Vugt, M. Verbeek, E. Westerhof, F. Wieschollek, and J. Zielinski, Nuclear Fusion **61**, 065001 (2021).
- [25] J.-Y. Ji and E. D. Held, Phys. Plasmas **21**, 042102 (2014).
- [26] J.-Y. Ji and E. D. Held, Phys. Plasmas **13**, 102103 (2006).
- [27] J.-Y. Ji and E. D. Held, Phys. Plasmas **16**, 102108 (2009).
- [28] R. Jorge, P. Ricci, and N. F. Loureiro, Journal of Plasma Physics **83**, 905830606 (2017).
- [29] R. Jorge, B. J. Frei, and P. Ricci, Journal of Plasma Physics **85**, 905850604 (2019).

- [30] J.-Y. Ji, E. D. Held, and C. R. Sovinec, Phys. Plasmas **16**, 022312 (2009).
- [31] J.-Y. Ji, H. Q. Lee, and E. D. Held, Phys. Plasmas **24**, 022127 (2017).
- [32] S. I. Braginskii, in *Reviews of Plasma Physics*, Vol. 1, edited by M. A. Leontovich (Consultants Bureau, New York, 1965) p. 205.
- [33] J.-Y. Ji and E. D. Held, Phys. Plasmas **22**, 062114 (2015).